MIT 3.071
Amorphous Materials

14: Characterizing the Amorphous State

Juejun (JJ) Hu

After-class reading list

- 3.012 X-ray diffraction
- 3.014 X-ray diffraction, Raman spectroscopy, and calorimetry

	Technique	Information
Structure	X-ray/electron/ neutron diffraction	Crystallinity, pair distribution function, medium range order
	X-ray absorption spectroscopy (XAS)	Local structure, electronic state
	Raman spectroscopy	Phonon spectra, structural clusters
	Nuclear magnetic resonance (NMR)	Local atomic configurations
Glass chemistry	Atomic emission spectroscopy (AES)	Elemental composition
	Energy-dispersive X-ray spectroscopy (EDX)	Elemental composition
	Infrared spectroscopy	Chemical bonding, impurity concentration, optical absorption
	X-ray photoelectron spectroscopy (XPS)	Valence state of constituents, electron density of states

	Technique	Information
Thermal analysis	Differential thermal analysis (DTA)	Glass transition temperature (T_g), crystallization (T_x)
	Differential scanning calorimetry (DSC)	Glass transition temperature (T_g), crystallization (T_x)
	Thermogravimetric analysis (TGA)	Chemical decomposition
	Thermomechanical analysis (TMA)	Thermal expansion, softening point, glass transition (T_g)
Electrical properties	Temperature-dependent electrical conductivity measurement	Conduction mechanism, activation energy, density of states at Fermi level (for VRH)
	Impedance spectroscopy (AC conductivity)	Conductivity, dielectric constant
	Electron paramagnetic resonance (EPR)	Defects (e.g. dangling bonds)

	Technique	Information
Mechanical and rheological behavior	Indentation	Hardness
	Ultrasonic wave propagation	Elastic modulus
	Fracture toughness test	Fracture toughness
	3/4-point bending test	Elastic modulus, flexural stress
	Viscometry	Viscosity
Optical properties	UV-Vis spectroscopy	Optical attenuation & absorption (100 dB/cm or higher), Tauc gap
	Ellipsometry	Refractive index dispersion
	Prism coupling	Refractive index (bulk and thin film), optical attenuation
	Optical fiber/waveguide transmission	Optical attenuation (< 100 dB/cm)
	Photoluminescence	Defect states

Diffraction techniques

Three dimensional visualization of diffraction intensities removed due to copyright restrictions. See Figure 2: "Serial Femtosecond Crystallography." CFEL Science, DESY.

Full 3-D x-ray structure factors of Photosystem I, a protein complex

Image courtesy:
Thomas White, CFEL

X-ray diffraction (XRD)

Figure of XRD line scan of amorphous and annealed Metglas foils removed due to copyright restrictions. See Figure 1: Li, M. et al. "Giant Magnetoelectric Effect in Self-biased Laminates Under Zero Magnetic Field." *Appl. Phys. Lett.* 102, no. 082404 (2013): 1-3.

Crystals:

- Strong scattering
- Localized, intense peaks

Glass:

- Weak scattering
- Broad scattering background across the entire reciprocal space

Appl. Phys. Lett. **102**, 082404 (2013)

X-ray diffraction in solids

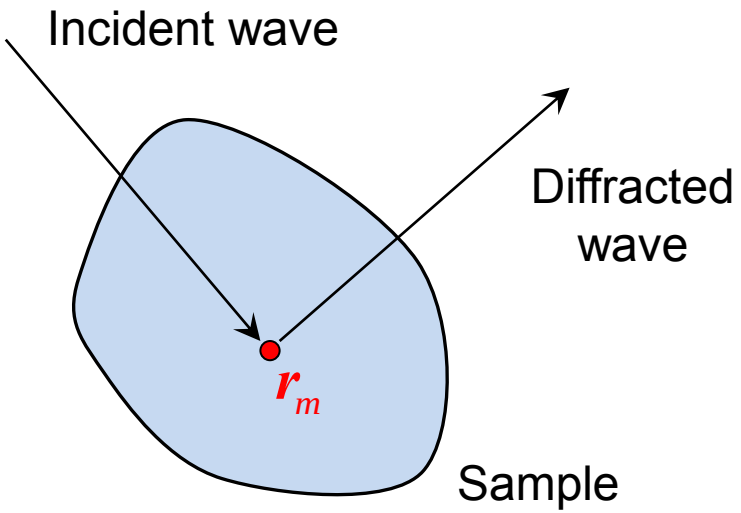

r_m : position vector of atom m

Assumptions:

- Approximate incident and diffracted X-ray as mono-chromatic plane waves
- Elastic scattering: wavelength of X-ray remains the same after scattering
- Neglect X-ray attenuation in the solid sample

X-ray diffraction by a single atom m

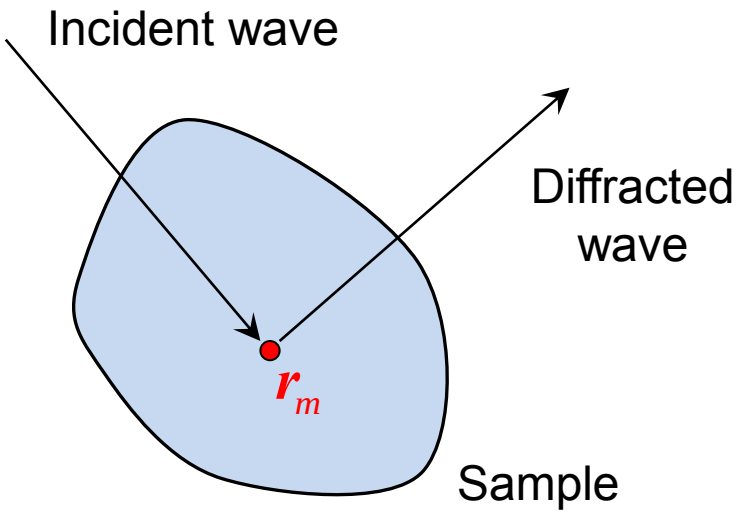

$\boldsymbol{E}$: field amplitude of incident X-ray

$\boldsymbol{k}_i$: wave vector of incident X-ray

$\boldsymbol{k}_s$: wave vector of scattered X-ray

f_m : scattering factor of atom m

$\mathbf{Q} = \boldsymbol{k}_s - \boldsymbol{k}_i$: scattering vector

- Complex amplitude of incident wave:

$$\boldsymbol{E}_i(\boldsymbol{r}) = \boldsymbol{E}\exp(i\boldsymbol{k}_i \cdot \boldsymbol{r})$$

- Field amplitude of the incident wave at $\boldsymbol{r}_m$:

$$\boldsymbol{E}_i(\boldsymbol{r}_m) = \boldsymbol{E}\exp(i\boldsymbol{k}_i \cdot \boldsymbol{r}_m)$$

- Complex amplitude of wave scattered by atom m:

$$\boldsymbol{E}_s(\boldsymbol{r}) \propto \boldsymbol{E}\exp(i\boldsymbol{k}_i \cdot \boldsymbol{r}_m) \times \exp\left[i\boldsymbol{k}_s \cdot (\boldsymbol{r} - \boldsymbol{r}_m)\right] = f_m \exp(-i\mathbf{Q} \cdot \boldsymbol{r}_m)$$

X-ray diffraction in solids

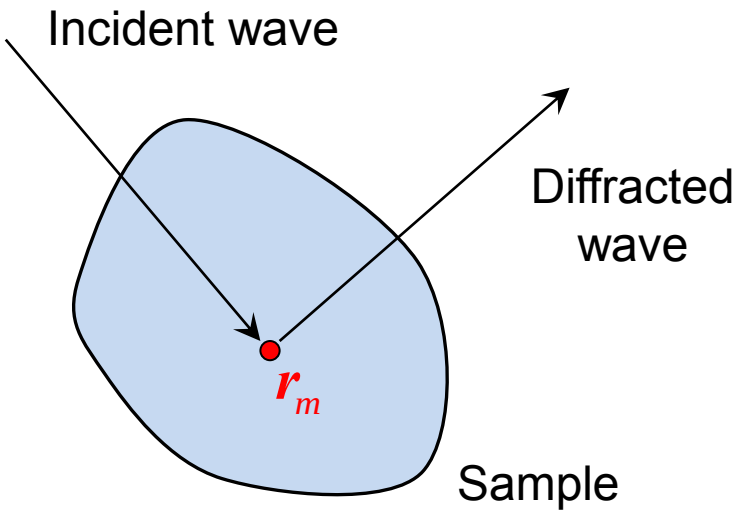

$S(\mathbf{Q})$: (static) structure factor

N : total number of atoms in the sample

- Total scattered amplitude from the sample :

$$\sum_m f_m \exp\left(-i\mathbf{Q}\cdot\boldsymbol{r}_m\right)$$

- Total scattered intensity:

$$I = \left|\sum_m f_m \exp\left(-i\mathbf{Q}\cdot\boldsymbol{r}_m\right)\right|^2$$

$$= \sum_m f_m \exp\left(-i\mathbf{Q}\cdot\boldsymbol{r}_m\right)$$

$$\times \sum_n f_n^* \exp\left(i\mathbf{Q}\cdot\boldsymbol{r}_n\right)$$

$$= S(\mathbf{Q}) \times N\left\langle f_m\right\rangle^2$$

X-ray diffraction in crystals

- The condition for a Bragg peak to appear is:

$$2d \sin\theta = \lambda$$

or: $\mathbf{Q} = \boldsymbol{k}_s - \boldsymbol{k}_i = \boldsymbol{G}_{hkl}$

- The Bragg peak intensity scales with:

$$\left| \sum_j f_j e^{-i\mathbf{Q}\cdot\mathbf{r}_j} \right|^2$$

where the sum is over all atoms in a unit cell

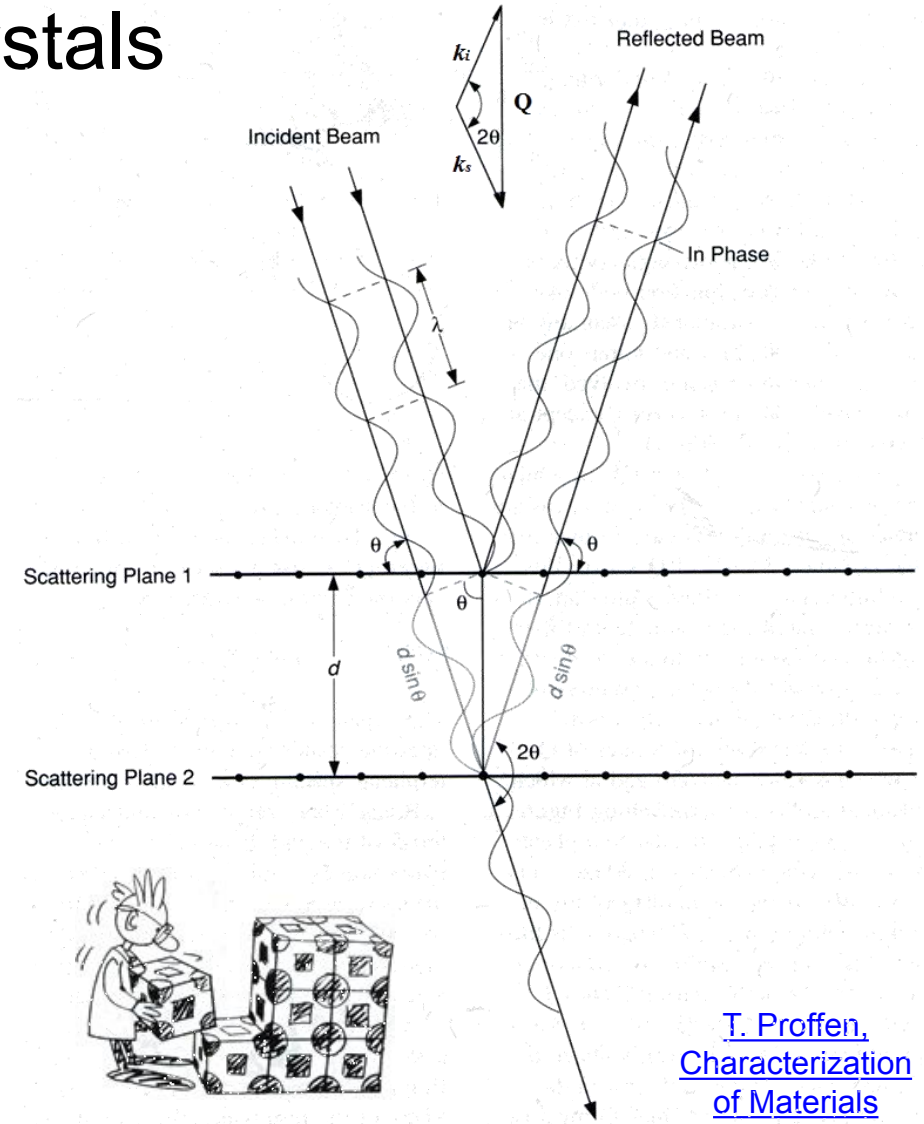

Unit cell: the repeating unit of a crystal

T. Proffen, Characterization of Materials using the PDF

Quantitative description of glass structure

- Structural descriptions of amorphous materials are always statistical in nature
- Pair distribution function (PDF): $g(r)$
  - Consider an amorphous material with an average number density of atom given by:

    $\rho = N/V$ N : number of atoms V : material volume
  - The number density of atoms at a distance r from an origin atom is given by $\rho \cdot g(r)$
  - When $r \to 0, g \to 0$
  - When $r \to \infty, g \to 1$

PDFs of ideal (hard sphere) crystals vs. glasses

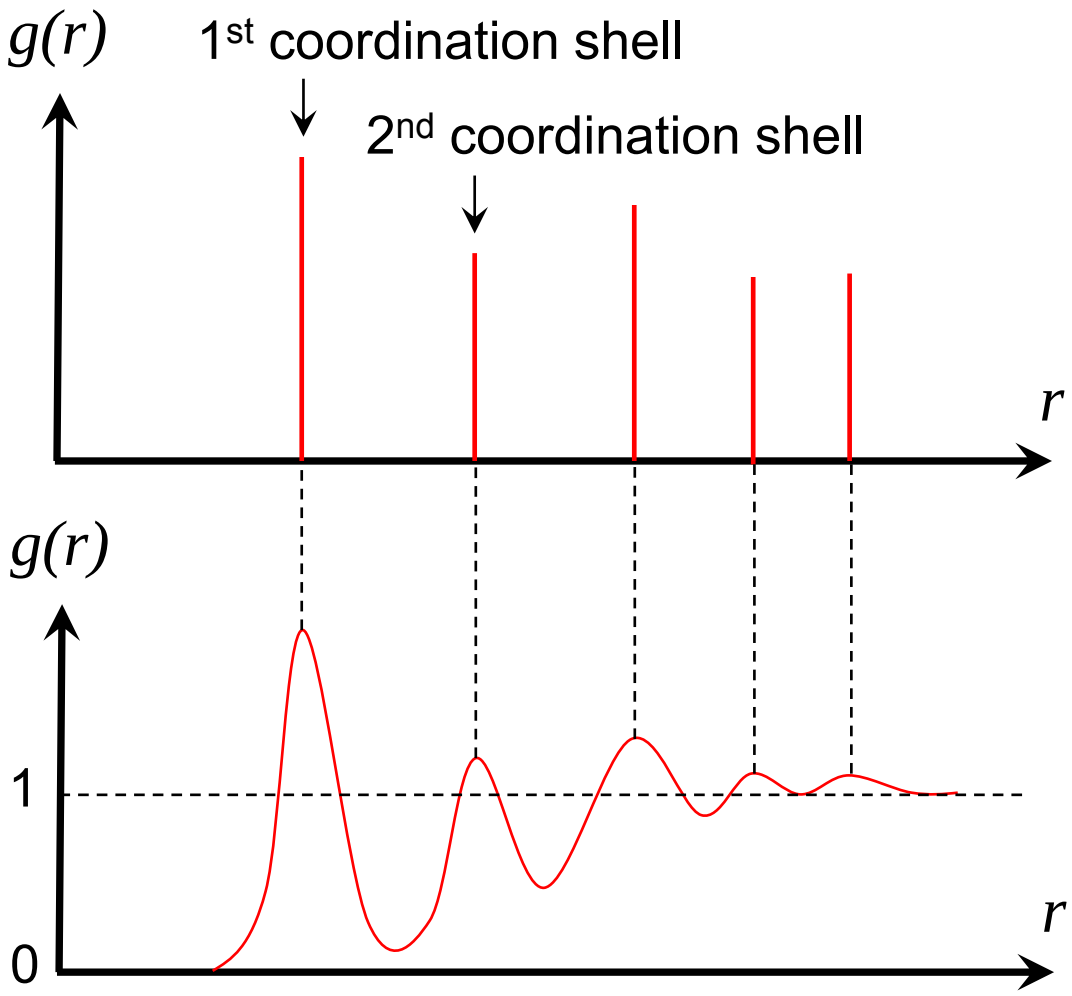

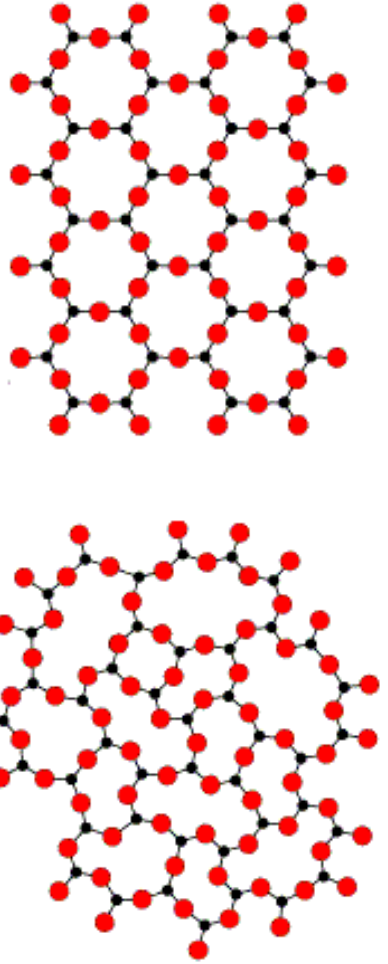

Mathematical description of PDF

- Probability density for finding an atom at $\boldsymbol{r}$:

$$\rho^{(1)}(\boldsymbol{r}) = \left\langle \sum_{m}^{N} \delta(\boldsymbol{r} - \boldsymbol{r}_m) \right\rangle = \rho$$ Homogeneous solid

- Probability density for finding an atom pair at $\boldsymbol{r}$ and $\boldsymbol{r}'$:

$$\rho^{(2)}(\boldsymbol{r}, \boldsymbol{r}') = \left\langle \sum_{m}^{N} \sum_{n \neq m}^{N} \delta(\boldsymbol{r} - \boldsymbol{r}_m) \delta(\boldsymbol{r}' - \boldsymbol{r}_n) \right\rangle = \rho^{(2)}(|\boldsymbol{r} - \boldsymbol{r}'|)$$

Homogeneous, isotropic solid

- Pair distribution function:

$$g(r) = \frac{1}{\rho^2} \rho^{(2)}(|\boldsymbol{r} - \boldsymbol{r}'|) = \frac{V^2}{N^2} \rho^{(2)}(|\boldsymbol{r} - \boldsymbol{r}'|)$$

Structure factor of isotropic amorphous solids

$$S(\mathbf{Q}) = \frac{1}{N\langle f_m \rangle^2} \times \left\langle \sum_m^N f_m \exp(-i\mathbf{Q}\cdot\mathbf{r}_m) \times \sum_n^N f_n^* \exp(i\mathbf{Q}\cdot\mathbf{r}_n) \right\rangle$$

$$= \frac{1}{N} \times \left\langle \sum_m^N \sum_n^N \left[\exp(-i\mathbf{Q}\cdot\mathbf{r}_m) \times \exp(i\mathbf{Q}\cdot\mathbf{r}_n) \right] \right\rangle$$

$$= 1 + \frac{1}{N} \left\langle \iint \left\{ \exp\left[-i\mathbf{Q}\cdot(\mathbf{r}-\mathbf{r}')\right] \times \sum_m^N \sum_{n\neq m}^N \delta(\mathbf{r}-\mathbf{r}_m)\delta(\mathbf{r}'-\mathbf{r}_n) \right\} d\mathbf{r}d\mathbf{r}' \right\rangle$$

$$= 1 + \frac{1}{N} \iint \left\{ \exp\left[-i\mathbf{Q}\cdot(\mathbf{r}-\mathbf{r}')\right] \times \rho^{(2)}(\mathbf{r},\mathbf{r}') \right\} d\mathbf{r}d\mathbf{r}'$$

$$= 1 + \rho \int \left[\exp(-i\mathbf{Q}\cdot\mathbf{r}) \times g(r) \right] d\mathbf{r} \qquad \text{where } r = |\mathbf{r}-\mathbf{r}'|$$

In isotropic solids structure factor is related to the Fourier transform of PDF

Debye scattering equation

- Isotropic amorphous media:

$$S(\mathbf{Q}) = 1 + \rho \int \left[\exp(-i\mathbf{Q}\cdot\boldsymbol{r}) \times g(r) \right] d\boldsymbol{r}$$

$$= 1 + 4\pi\rho \int_0^\infty r^2 g(r) \frac{\sin(\mathrm{Q}r)}{\mathrm{Q}r} \cdot dr \qquad \text{where } \mathrm{Q} = |\mathbf{Q}| = \frac{4\pi}{\lambda}\sin\theta$$

- The inverse transform:

$$g(r) = 1 + \frac{1}{2\pi^2\rho} \int_0^\infty \left[S(\mathrm{Q}) - 1 \right] \cdot \mathrm{Q}^2 \frac{\sin(\mathrm{Q}r)}{\mathrm{Q}r} \cdot d\mathrm{Q}$$

XRD spectra can be used to infer PDF of isotropic amorphous solids

Solving PDF from experimental XRD spectra

Raw XRD data → Data correction → Structure factor normalization → Transform to real space

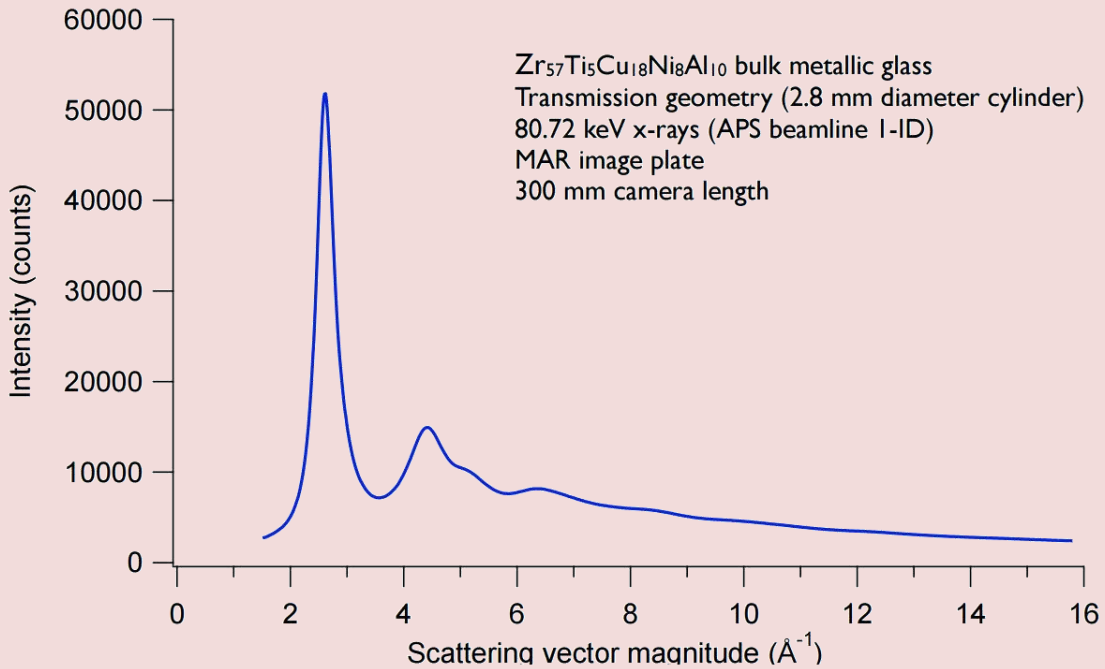

Data from T. C. Hufnagel, Johns Hopkins University

Solving PDF from experimental XRD spectra

Raw XRD data → Data correction → Structure factor normalization → Transform to real space

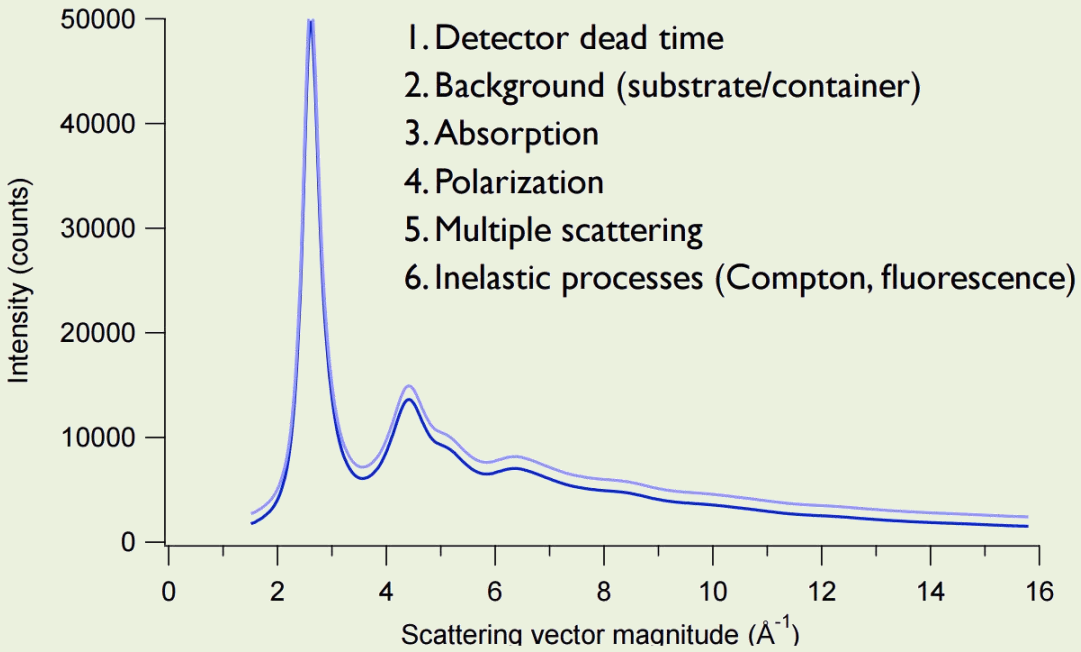

1. Detector dead time
2. Background (substrate/container)
3. Absorption
4. Polarization
5. Multiple scattering
6. Inelastic processes (Compton, fluorescence)

Data from T. C. Hufnagel, Johns Hopkins University

Solving PDF from experimental XRD spectra

Raw XRD data → Data correction → Structure factor normalization → Transform to real space

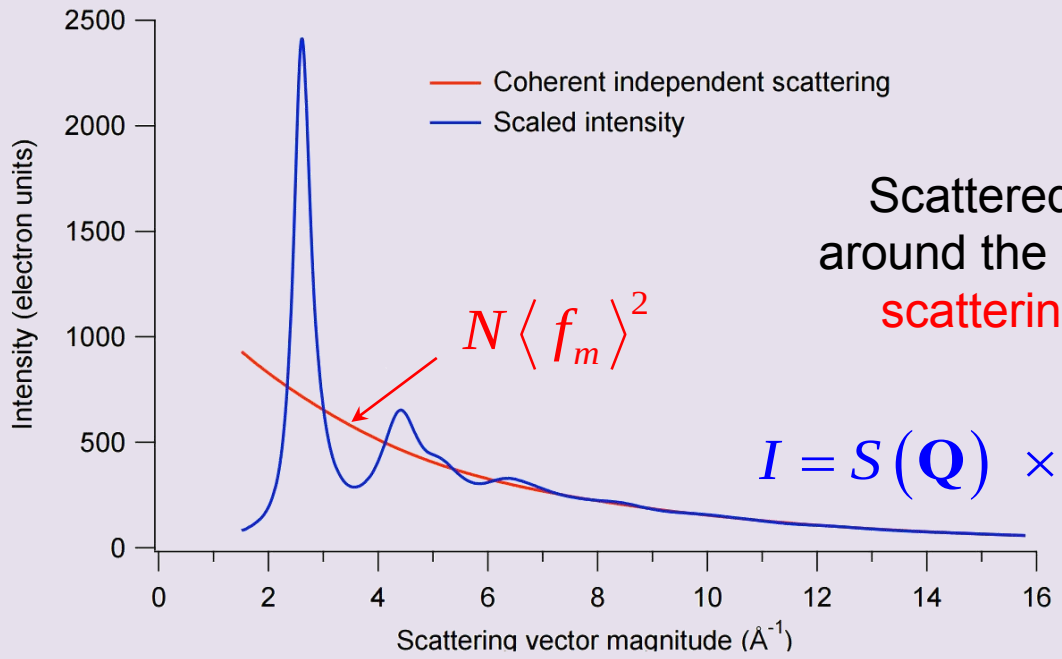

Scattered intensity oscillates around the coherent independent scattering at large Q values

$$I = S(\mathbf{Q}) \times N\langle f_m \rangle^2$$

Data from T. C. Hufnagel, Johns Hopkins University

Solving PDF from experimental XRD spectra

Raw XRD data → Data correction → Structure factor normalization → Transform to real space

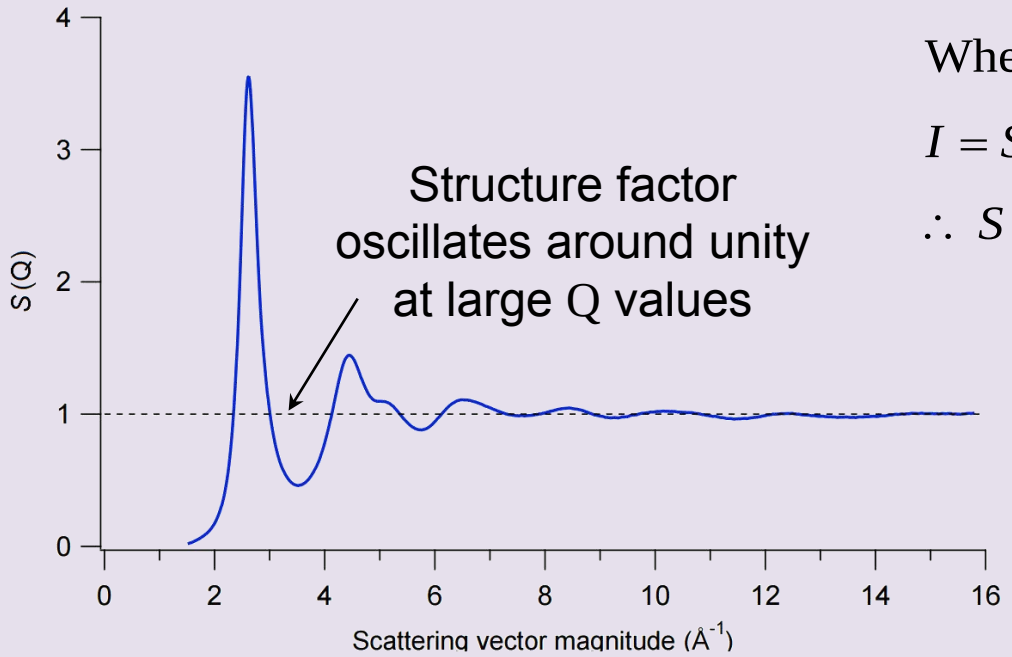

When $Q \to \infty$

$$I = S(\mathbf{Q}) \times N\langle f_m \rangle^2 \to N\langle f_m \rangle^2$$

$$\therefore\ S(\mathbf{Q}) \to 1$$

Data from T. C. Hufnagel, Johns Hopkins University

Solving PDF from experimental XRD spectra

Raw XRD data → Data correction → Structure factor normalization → Transform to real space

$$g(r) = 1 + \frac{1}{2\pi^2 \rho} \int_0^{Q_{max}} \left[S(Q) - 1 \right] \cdot Q^2 \frac{\sin(Qr)}{Qr} \cdot dQ$$

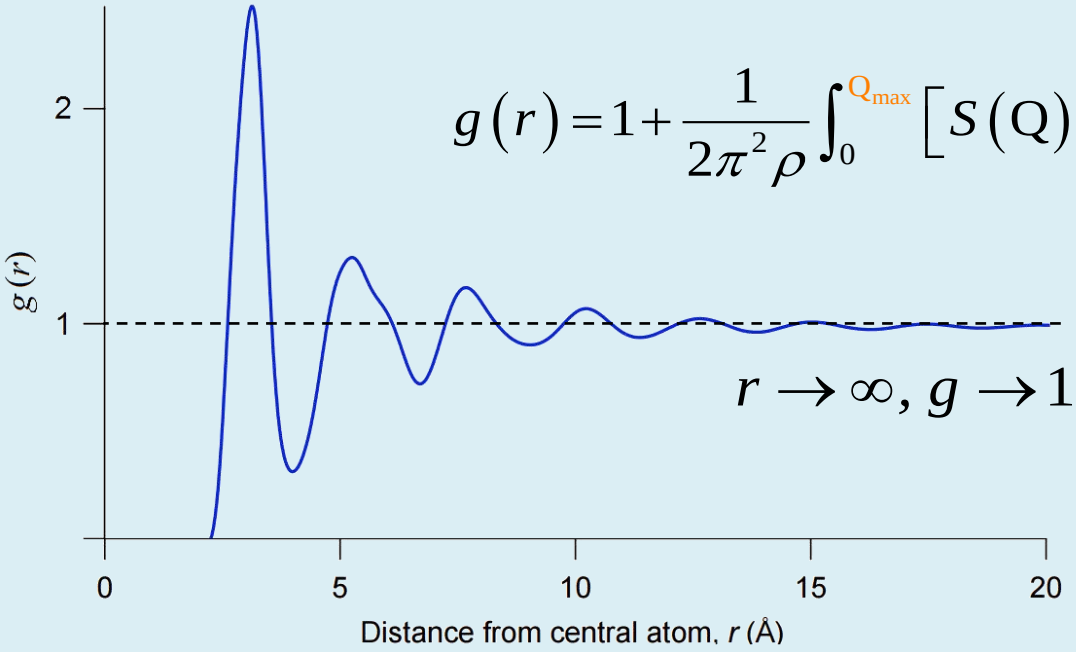

Data from T. C. Hufnagel, Johns Hopkins University

Solving PDF from experimental XRD spectra

- Sources of error
  - $S(Q)$ data truncation error
  - X-ray photon shot noise
  - Finite resolution
- Mitigation strategies
  - Use Mo ($\lambda_{K\alpha}$ = 0.71 Å) or Ag ($\lambda_{K\alpha}$ = 0.56 Å) sources instead of Cu source ($\lambda_{K\alpha}$ = 1.54 Å)
  - Increase collection time

[Determination of Pair Distribution Functions (PDF)](#) from Bruker

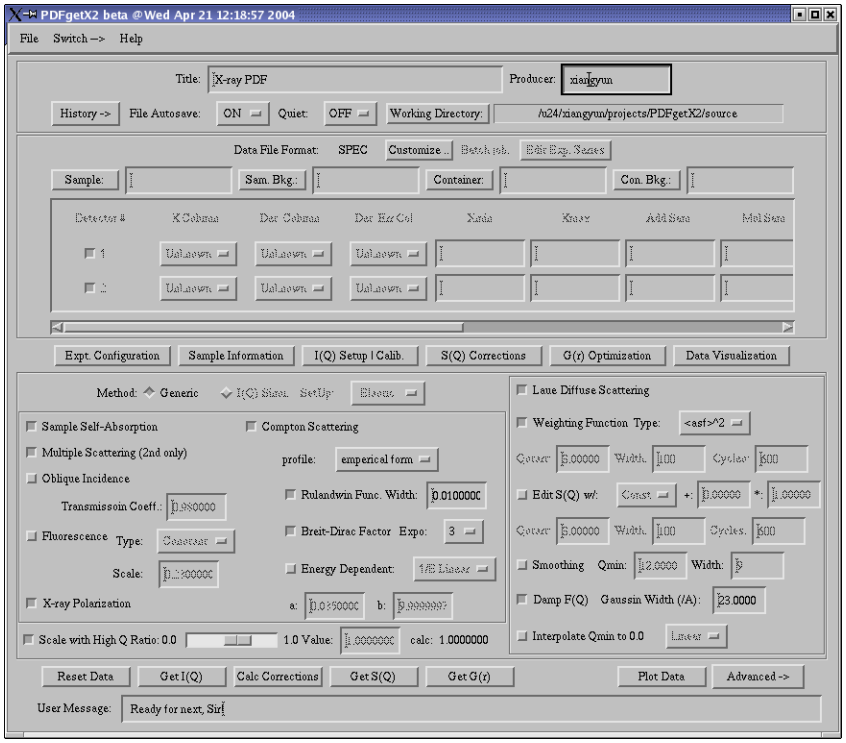

[PDFGetX2 homepage](#)

J. Appl. Cryst. **37**, 678 (2004)

Electron and neutron diffraction

- Electron diffraction
  - Much smaller wavelength (e.g. $\lambda \sim 2$ pm for 300 keV electrons)
  - Small spot size (e.g. in the case of SAED)
- Neutron diffraction
  - Interacts with nuclei rather than electrons
  - Can discriminate neighboring elements or isotopes
  - Can detect light elements

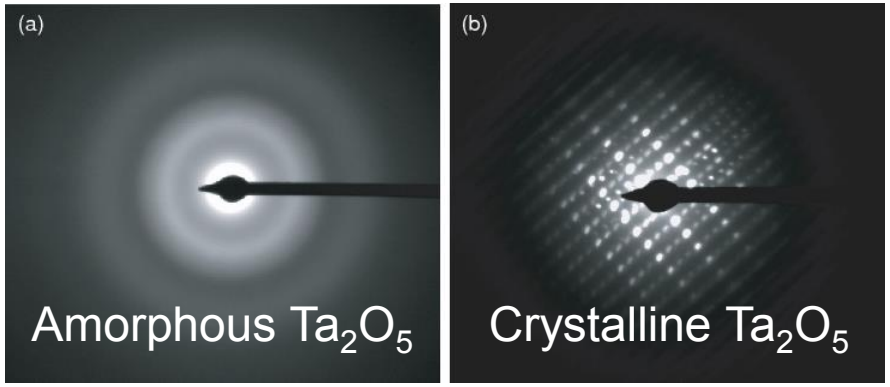

Electron diffraction patterns

Class. Quantum Grav. **27**, 225020 (2010)

Raman spectroscopy

Chandrasekhar Venkata Raman
(1888-1970)

When asked about his inspiration behind the Nobel Prize winning optical theory, Raman said he was inspired by the "wonderful blue opalescence of the Mediterranean Sea" while he was going to Europe in 1921.

Raman spectroscopy

- Raman scattering: inelastic and nonlinear interaction of photons with phonons
  - Photon – phonon = Stokes line
  - Photon + phonon = anti-Stokes line

laser-detect.com/technology-methods/

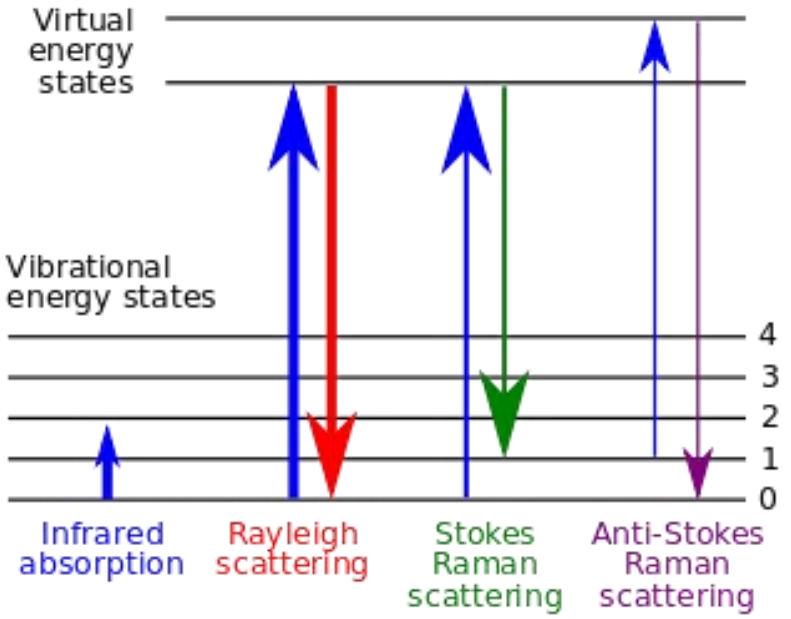

Raman spectra of amorphous materials

- Amorphous materials typically have broad Raman peaks
  - Dispersion of local structures and phonon energy

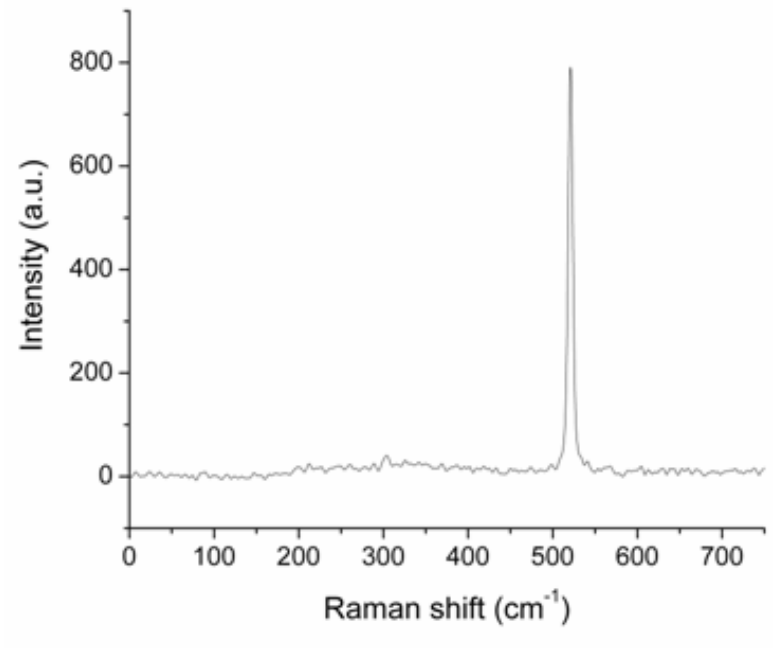

Raman spectrum of c-Si

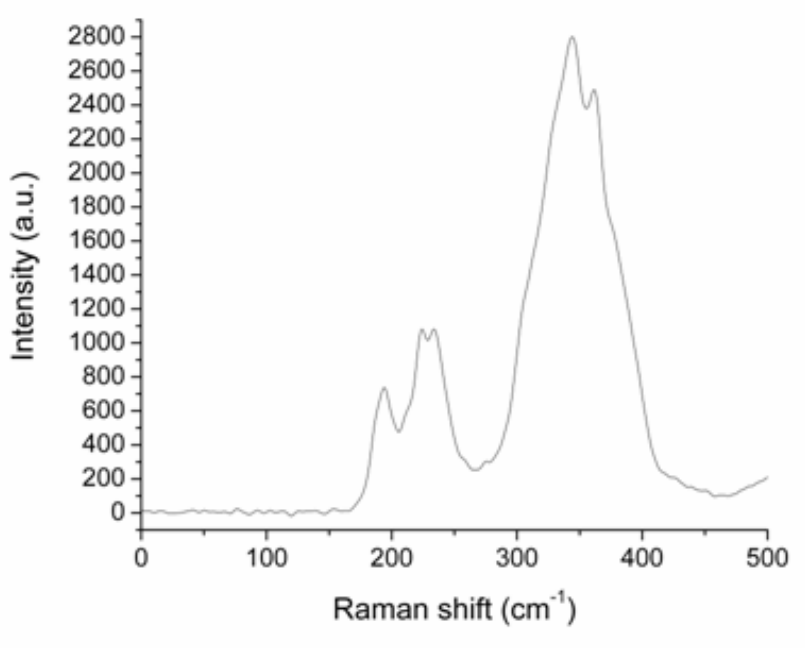

Raman spectrum of As_2S_3 glass

Example: Raman analysis of TeO_2-Bi_2O_3-ZnO glass

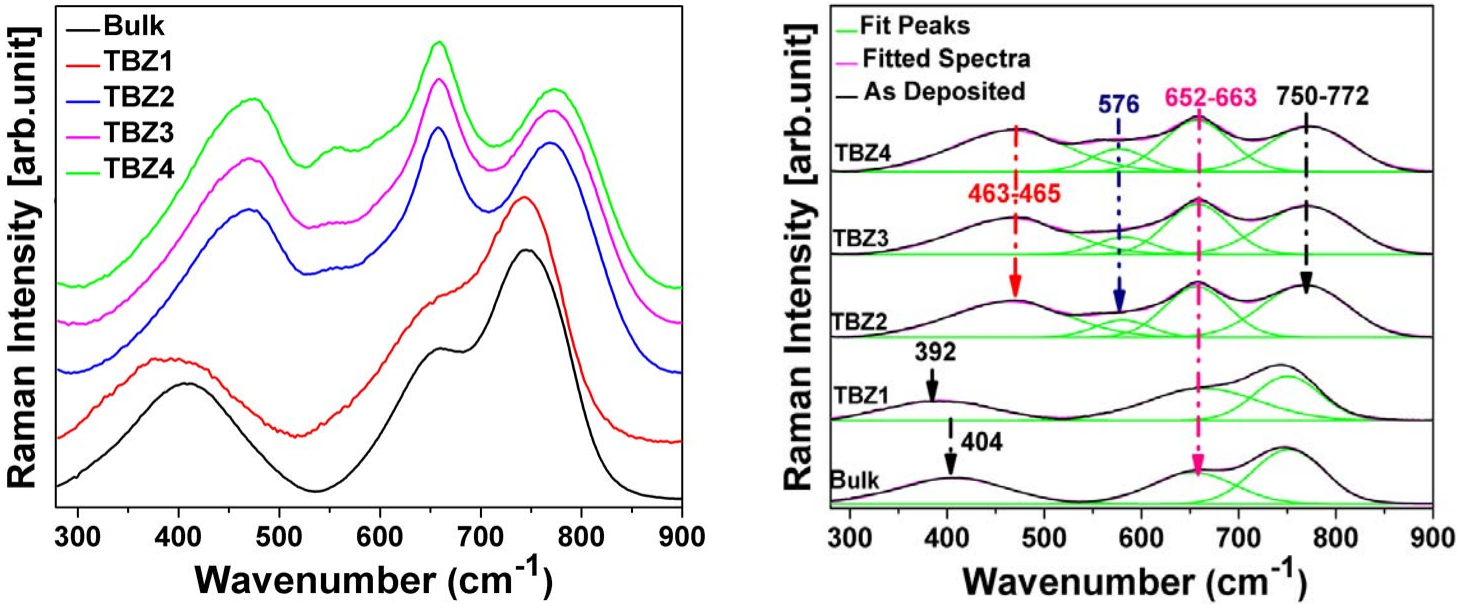

Raman band (cm^{-1})	Assignment
392 -404	Bending mode of Te-O-Te linkage in TeO_3 network backbone
463 - 465	Bending mode of O-Te–O linkages in TeO_4 network backbone
576	Soda-lime glass substrate contribution
656 - 657	Vibration of the Te-O bonds in TeO_4 trigonal bipyramid with bridging oxygen
750 - 772	Stretching of Te-O or Te=O which contain non-bridging oxygen (NBO) in TeO_{3+1} or TeO_3

J. Am. Ceram. Soc. **98**, 1731 (2015)

Calorimetry (thermal analysis)

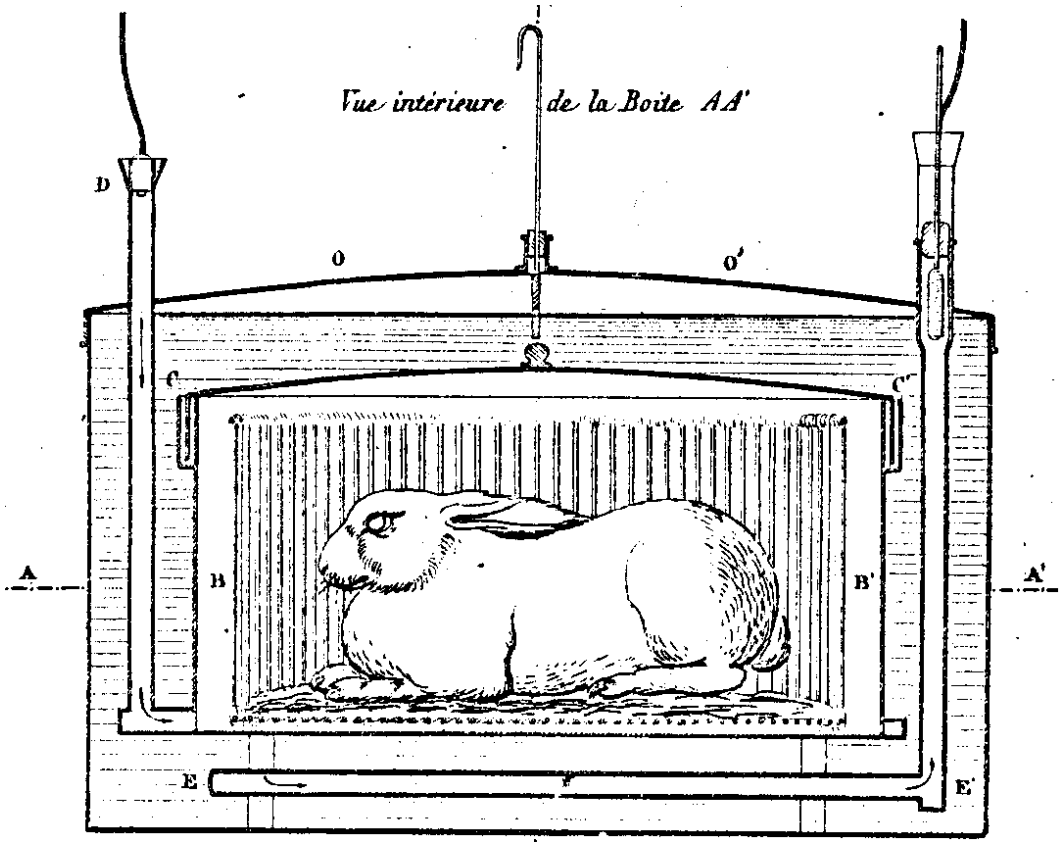

Courtesy of Gallica.
Source: Dulong, "Mémoire sure la chaleur animale." *Annales de chimie et de physique* SER3, T1 (1841): 440-455 (plate p. iii).

Apparatus for measuring animal heat

Pierre Louis Dulong, *Annales de chimie et de physique* (1841)

Differential Scanning Calorimetry (DSC)	Differential Thermal Analysis (DTA)
Both techniques involve a sample and an inert reference with known heat capacity both undergoing controlled heating or cooling	
Heating rate is kept constant for both the sample and the reference, and **heat flow** to the sample minus heat flow to the reference is recorded	Both the sample and the reference undergo identical **thermal cycle** and **temperature difference** between sample and reference is recorded
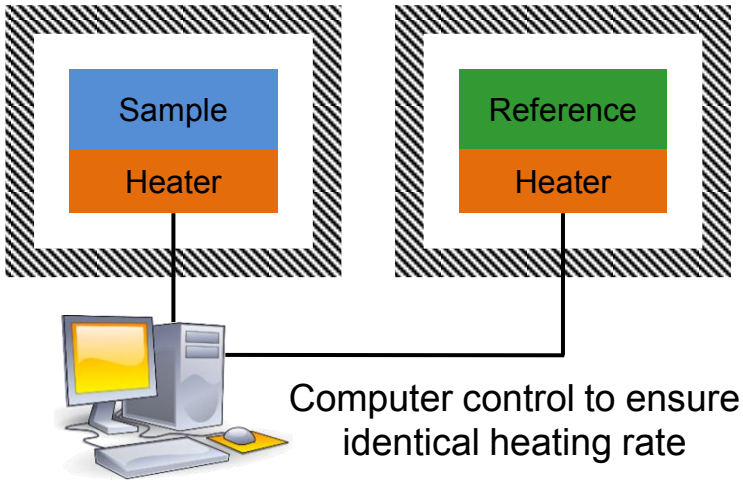	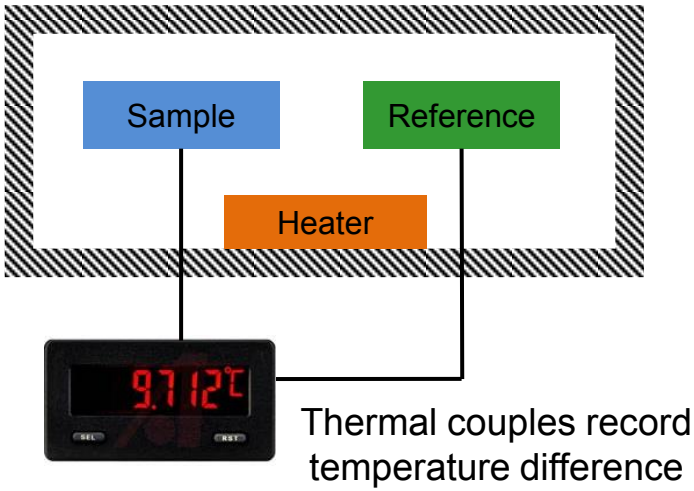

Differential scanning calorimetry of glass materials

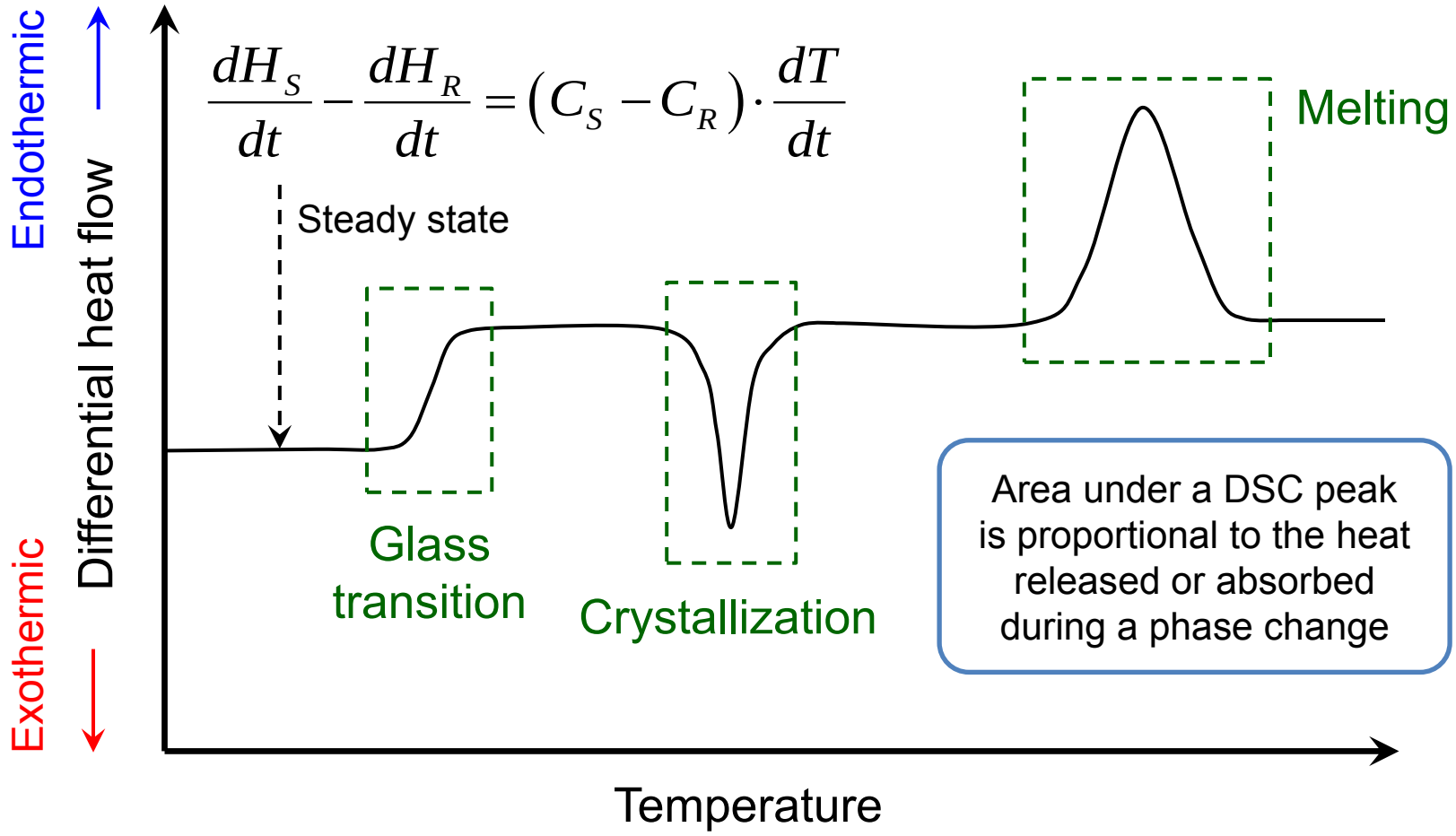

Glass transition regime behavior in DSC

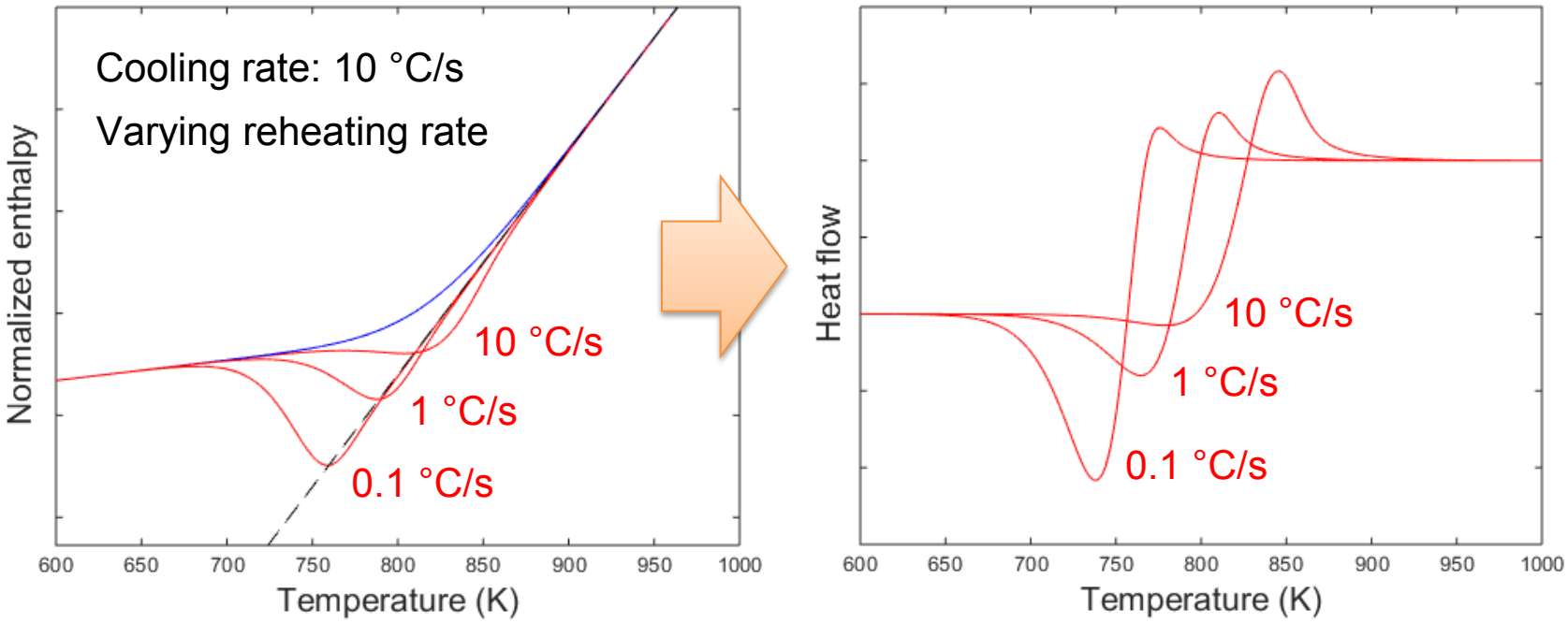

Shape of DSC curve at the glass transition regime depends on heating rate and the sample's thermal history

Differential thermal analysis of glass materials

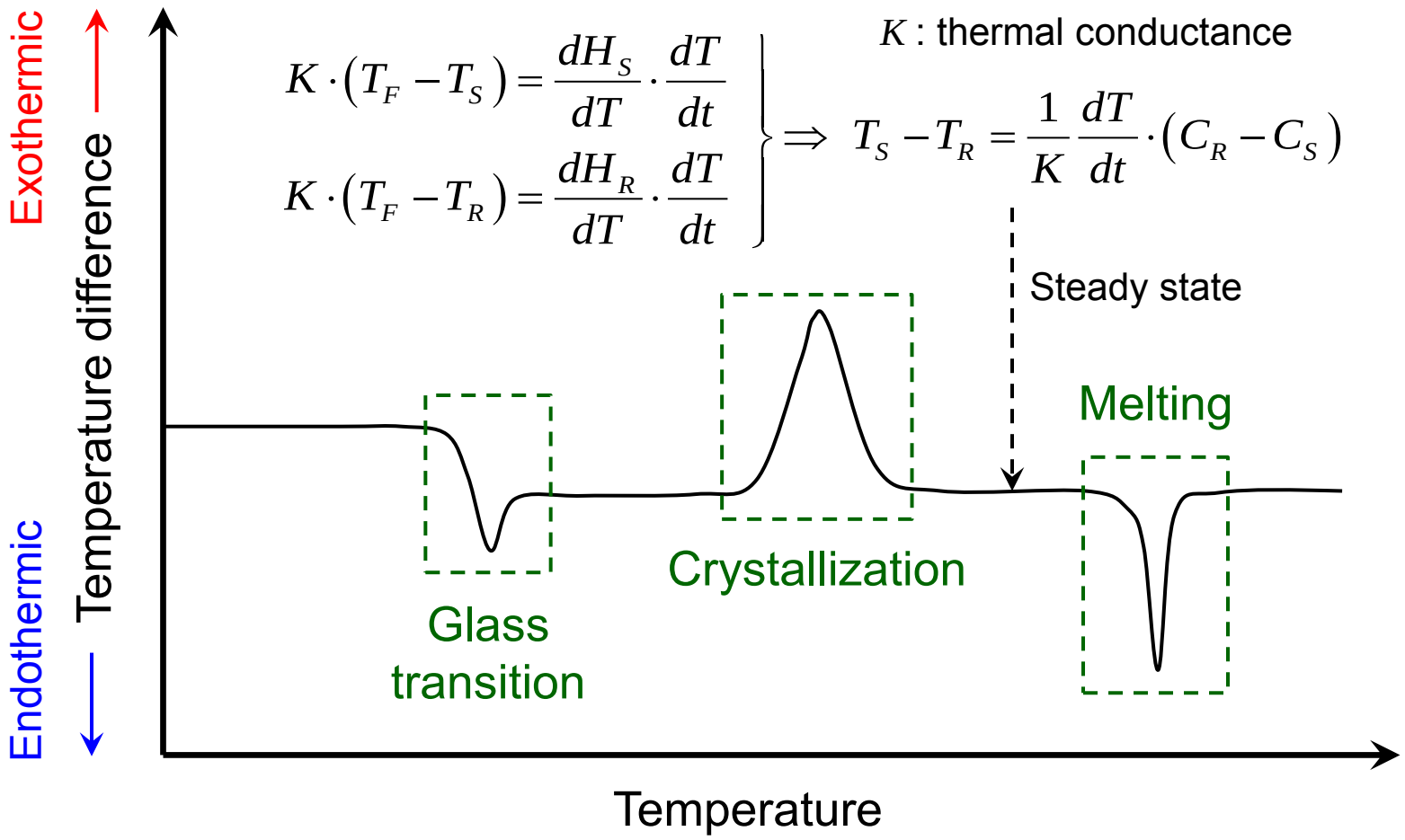

Evaluation of glass forming ability

Figure removed due to copyright restrictions. See Figure 1: Hrubý, A. "Evaluation of glass-forming tendency by means of DTA." *Czech. J. Phys. B* 22 (1972): 1187-1193.

- FOM for glass stability:

  $$\left(T_x - T_g\right) \Big/ \left(T_m - T_x\right)$$

  Hruby coefficient

- Addition of Si increases glass melt viscosity and improves glass forming ability

  Czech. J. Phys. B **22**, 1187 (1972)

Summary

- Diffraction
  - Debye diffraction equation: relation between structure factor and PDF in homogeneous, isotropic amorphous solids
  - Solving PDF from experimentally measured XRD spectra: corrections and normalization
  - X-ray, electron, and neutron diffraction
- Raman spectroscopy
  - Broad Raman peaks: phonon energy dispersion
- Thermal analysis
  - DSC vs. DTA: data interpretation
  - Glass transition regime behavior

3.071 Amorphous Materials

Fall 2015